MODELLING OF LIQUID SPRAYS IN EXCITED JET USING LARGE EDDY SIMULATION

Artur Tyliszczak
Institute of Thermal Machinery,
Czestochowa University of Technology
Al. Armii Krajowej 21, 42-200 Czestochowa, Poland
atyl@imc.pcz.czest.pl

Lukasz Kuban
Institute of Thermal Machinery,
Czestochowa University of Technology
Al. Armii Krajowej 21, 42-200 Czestochowa, Poland
lkuban@imc.pcz.czest.pl

ABSTRACT

This paper presents the results of LES simulations of the non-evaporating liquid spray injected in the center of the gaseous excited and non-excited jets. The spray is modelled using stochastic approach including stochastic droplets dispersion caused by the turbulent motion. We considered different velocities and different angles of the droplets injection. The numerical algorithm for the gas phase is based on the projection method, time integration is performed by low storage Runge-Kutta scheme and for spatial discretization we applied high order compact scheme combined with the Fourier pseudospectral method.

INTRODUCTION

Turbulent flow control plays an important role in a wide variety of technological applications due to possible increase in process efficiency and safety. The turbulent jets are examples of the flow problems for which the important applications are the fuel injection in engines, aircraft propulsion systems or atomizers. Active jet control was first reported by (Crow and Champagne, 1971) who observed that application of suitable excitation (forcing) at the jet inlet intensifies mixing phenomena. From that time many researches focused on this method of flow control as it in fact allows to increase the mixing and transport processes. Spectacular example of the application of the flow control are the bifurcating jets (Reynolds et al., 2003) occurring under particular excitation conditions. They may be characterized as jets which split downstream the potential core into two separate well defined streams. Experimental works (Reynolds et al., 2003; Parekh et al., 1988) concerning isothermal bifurcating jets showed that in this type of flows the frequency of excitation is a crucial parameter determining the type of instability (bi-, trifurcating, blooming jets). The resulting flowfield, dependent on the excitation parameters may be of crucial importance for many applications. In this work we analyze the liquid-droplet flows, for which the mixing efficiency is very often connected directly to the overall process efficiency in many applications. For example in a case of reacting flows (e.g. combustion) the vaporization rate, responsible for gaseous fuel production, is strictly related to the mixing processes. Thus, controlling the mixing process could effectively increase efficiency of combustion. In this work we will perform numerical simulation of spray in turbulent excited jets using Large Eddy Simulation. Due to inertia of liquid droplets the behavior of the excited jets with spray may be different from that of pure jets. We tried to answer the following questions: how the droplets influence the excited jets and whether (or to what extent) they follow the flowfield? The modeling of spray is performed by application of probability density function (PDF) which describes droplets properties (position, velocity, size, etc.). We follow the approach of (Jones and Sheen, 1999) where the stochastic method is applied instead of solving transport equation for PDF.

GOVERNING EQUATIONS AND NUMERICAL METHOD

In this work the gas phase is treated as the isothermal and constant density. These assumptions greatly simplify the problem, the continuity and Navier-Stokes equations have the form proper for the incompressible flows and there is no need to solve the energy equation. The drag force induced by droplets is the only term responsible for coupling between the gas and liquid phase. In the framework of Large Eddy Simulation the filtered continuity and the Navier-Stokes equations are given as:

$$\frac{\partial \bar{u}_j}{\partial x_j} = 0 \tag{1}$$

$$\frac{\partial \bar{u}_i}{\partial t} + \frac{\partial \bar{u}_i \bar{u}_j}{\partial x_j} = -\frac{1}{\rho}\frac{\partial \bar{p}^{(1)}}{\partial x_i} + \frac{1}{Re}\frac{\partial \bar{\tau}_{ij}}{\partial x_j} + \mathcal{T}_{ij}^{SGS} + F_D \tag{2}$$

where the $(\bar{\cdot})$ symbol denotes filtered variable (Sagaut, 2001), τ_{ij} is the viscous stress tensor and $\mathcal{T}_{ij}^{SGS}$ is the subgrid tensors modeled using filtered structure function model (Ducros et al., 1996; Metais et al., 1999). Symbol F_D represents the drag force induced by droplets.

The numerical algorithm applied for solution of gaseous phase is based on the projection method (Fletcher, 1991) which determines the pressure field and divergence free velocity field. The spatial discretization is performed with 6^{th} order collocated compact difference scheme (Lele, 1992) in the jet streamwise direction combined with the Fourier pseudospectral method (Canuto et al., 1988), dealiased according to 3/2 low, in directions perpendicular to the jet axis. The viscous term is computed in non-conservative form involving the I^{st} and II^{nd} order derivative operators - this approach reduces the grid-to-grid oscillations arising due to

two consecutive applications of the I^{st} derivative compact differences operator. The time integration is performed by low storage three-stage Runge-Kutta method (Williamson, 1980), where the projection step is solved in each stage. The applied code reveals to be very accurate in various type of jet flows including natural and excited jets (Tyliszczak and Boguslawski A., 2006; Tyliszczak and Boguslawski, 2007).

Spray modelling

The turbulent dispersion of liquid spray can be modelled by the evolution of joint probability density function (PDF) of the spray properties, where the spray velocity is proportional to the velocity of gas phase which acts on the droplets. We assume two phase problem in which sets of conservation equations are written for each phase, where in general case it is presumed that the spray can be described uniquely in terms of a single droplet dimension r, the droplet velocity v_j, the droplet number density n and droplet temperature θ. In order to describe the statistical properties of the spray the joint probability density function, $P(r, n, v_j, x, t)$ for the spray properties is introduced which evolves according to the equation of the form:

$$\frac{\partial P}{\partial t}+v_j\frac{\partial P}{\partial x_j}+\frac{\partial}{\partial v_j}(f_j P)+\frac{\partial}{\partial n}(\dot{N}P)+\frac{\partial}{\partial r}(\dot{R}P)+\frac{\partial}{\partial \theta}(\dot{\Theta}P)=0 \tag{3}$$

where:
f_j - is the force per unit mass exerted on the droplets by the surrounding gas;
$\dot{N}$ - dn/dt, is the rate of increase of droplet number density through liquid film and droplet breakup and coalescence;
$\dot{R}$ - dr/dt, is the rate of change of droplet size due to evaporation;
$\dot{\Theta}$ - $d\theta/dt$, rate of change of droplet temperature arising from heat transfer from the surroundings gas phase.

Equation (3) involves ten independent dimensions and therefore the solution of this equation would be extremely expensive computationally applying finite difference type of approximation. Fortunately, the hyperbolic nature of the equation (3) allows to solve its separate characteristic equations for the properties of the stochastic particles. In case of the isothermal flows with assumed constant droplet density number the characteristic equations reduce to the solution of equations for position and velocity of the p-th particles. The movement of the stochastic particles is mostly determined by the gas phase velocity, however droplet motion is also affected by stochastic forces arising from the turbulent motions of the gas phase. In this case the equations of motion of particles including random dispersion can be written as (Jones and Sheen, 1999):

$$d\hat{v}_j^{(p)}=\frac{1}{\tau_p}\left(\bar{u}_j-\hat{v}_j^{(p)}\right)dt+\sqrt{C_o k/\tau_p dt}\;\xi_j \tag{4}$$

$$\frac{d\hat{x}_j^{(p)}}{dt}=\hat{v}_j^{(p)} \tag{5}$$

where $(\hat{\cdot})$ indicates property of the p-th particle. The last term on the right hand side of Eq.(4) is derived (Jones and Sheen, 1999) assuming that the stochastic forces are represented by the Wiener process. The empirical constant C_o has the value equal to one (Jones and Sheen, 1999). The turbulence kinetic energy, k is computed based on the LES filter width and resolved velocity field. The symbol ξ_j is an independent component of the random vector with zero mean and variance equal to one. The relaxation time of the particle is given as:

$$\tau_p=\left(\frac{3}{8}C_D\frac{\rho}{\rho_L}\frac{|\bar{u}_j-\hat{v}_j^{(p)}|}{\hat{r}^{(p)}}\right)^{(-1)} \tag{6}$$

where the drag coefficient, C_D is defined as:

$$C_D=\frac{24}{Re_p}(1+0.15Re_p^{0.687})\;\text{ for } Re_p\le 1000 \tag{7}$$

$$C_D=0.44\;\text{ for } Re_p>1000 \tag{8}$$

The Reynolds number Re_p of the particles is determined based on a particle diameter and the relative velocity of the particle with respect to the gas phase. The densities of the gas and liquid phase are denoted as ρ and ρ_L respectively. In this work the ratio of the liquid phase to the gas phase density is equal to 1000. The equations (4) and (5) have a form very similar to the classical Lagrangian equations for the motion of real droplets where the trajectories of representative droplets are tracked directly allowing to determine their position, velocity, etc.. In the PDF approach all dependent variables are random variables representing position in the 'spray properties' space. In this case particles are not real droplets but they are stochastic particles used only to represent the PDF by an ensemble average.

BOUNDARY CONDITIONS

The computational domain together with a schematic view of the jet and spray nozzle is shown in Fig.1. In performed computations we only considered the rectangular box $7D \times 12D \times 7D$ (D is the jet diameter) where at the inlet plane we specified the jet velocity profile and spray characteristic, i.e. particle velocities, angle of injection, droplets diameter distribution. The lateral boundaries of the computational domain are assumed periodic while the inlet boundary conditions for the gas phase are specified in terms of instantaneous velocity. The inlet boundary conditions for spray are discussed in the next subsection. At the outlet of the computational domain we applied the convective type boundary conditions. For each time step the instantaneous axial velocity is generally defined as:

$$u(\vec{x},t)=u_{mean}(\vec{x})+u_{noise}(\vec{x},t)+u_{excit}(\vec{x},t) \tag{9}$$

where the mean velocity $u_{mean}(\vec{x})$ is defined by hyperbolic-tangent profile (da Silva and Metais, 2002; Tyliszczak and Boguslawski, 2007).The fluctuating component of velocity $u_{noise}(\vec{x},t)$ is the random Gaussian noise adjusted (da Silva and Metais, 2002) to have turbulence level equal to 5% in the vicinity of the shear layer ($0.8 < r/R < 1.2$) and 1% in the region where $r \le 0.8$. The forcing component of the axial velocity is defined as:

$$u_{excit}(\vec{x},t)=A_a\sin\left(2\pi St_a\frac{U_1}{D}t\right)+ A_h\sin\left(2\pi St_h\frac{U_1}{D}t+\frac{\pi}{4}\right)\sin\left(\frac{\pi x}{R}\right) \tag{10}$$

which is a superposition of axial forcing (the first term) and helical/flapping forcing (the second term). The forcing amplitudes are A_a and A_h, the Strouhal numbers are defined as $St_a = f_a D/U_1$ and $St_h = f_h D/U_1$ where U_1 is the jet centerline velocity and f_a, f_h are the frequencies of axial and helical forcing respectively. The amplitudes of the forcing

were equal to 0.05% of the jet velocity, the Strouhal number of axial forcing was equal to 0.5 (close to the Struhal number of the preffered mode frequency - 0.44 in our simulations) and the ratio of the axial and helical Strouhal numbers (St_a/St_h) was equal to 2. These are the conditions causing bifurcations (Reynolds et al., 2003). Computations were performed for the Reynolds number equal to 10000 defined based on the jet axis velocity, jet nozzle diameter and jet viscosity.

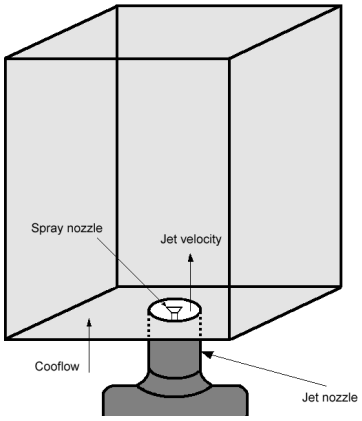

Figure 1: Schematic view of the computational domain together with sketched spray and jet nozzles.

Spray characteristic

The spray is injected in the center of the jet, the radius of the virtual cone is equal to the 1/2 of the jet radius. We analyzed two different angles of injection $\alpha_p = 30^o$ and $\alpha_p = 60^o$ - the angle of injection was gradually varying along the cone radius in such way that in the center of injection the velocity of the droplets was parallel to the velocity of the jet. Computations were performed for three values of the spray velocity: in the first case the modulus of spray velocity was equal to the jet velocity, i.e. $U_p = U_1$, then it was decreased to 10% and 5% of the jet velocity. In all cases the fluctuations of modulus of the spray velocity were assumed equal to 5%. The cartesian components of the spray velocity were computed depending on the cone radius and local angle determined randomly within the cone area. The diameters of the injected droplets were selected randomly from the modified Rosin-Rammler distribution (Lefebvre, 1989) with $SMD = 30$. In each time step the amount of injected particles (approximately 8000) resulted from the specified mass flow $Q = 1g/s$ and particle number density assumed equal to 15. The allowable numerical time-step was determined based on the maximum droplets velocity and cell size, the Runge-Kutta procedure for the gas phase was realized as the inner part between two succesive droplets injection.

RESULTS

Computational mesh consisted of $128 \times 120 \times 128$ uniformly spaced nodes. Comparing preliminary results obtained using this mesh with the results obtained on the mesh twice finer we did not observe any qualitative differences neither in the flowfield nor in the droplets distribution. For each case presented in this paper computations were run over $200D/U_1$ time units and averaging procedure started after transient flowfield development and was continued during the last $100D/U_1$ time units. Computations were performed on PC cluster using four processors and each run took 24 hours approximately - increase of the computational time caused computations of droplets position and velocity is about 40% comparing to the computations of the pure jets, i.e. without droplets.

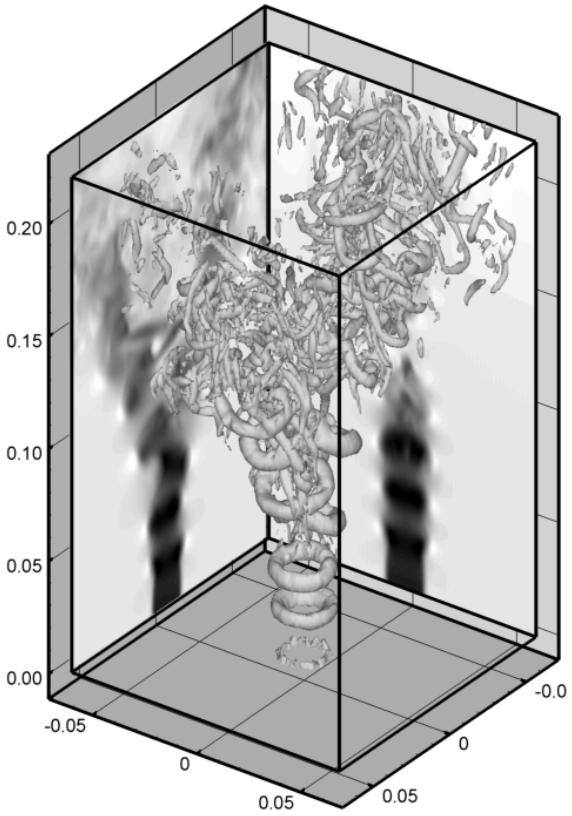

Figure 2: Instantaneous isosurface of Q parameter and contours of axial velocity in cross-ssection

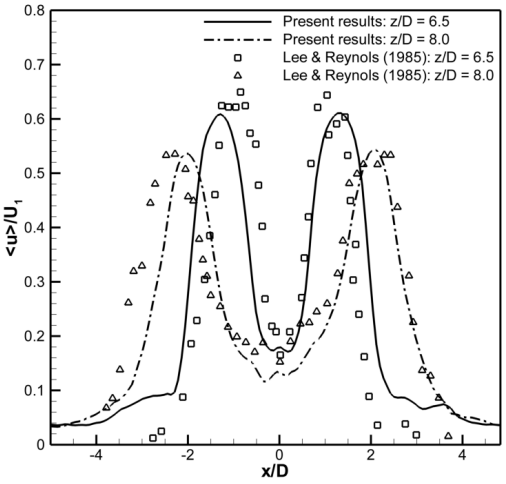

Figure 3: Mean axial velocity in bifurcating plane along the jet radius at 6.5 and 8.0 diameters from the inlet plane.

Sample results showing instantaneous isosurface of the Q parameter and contours of the axial velocity are shown in Fig. 2, where two branches of the bifurcating jet are well

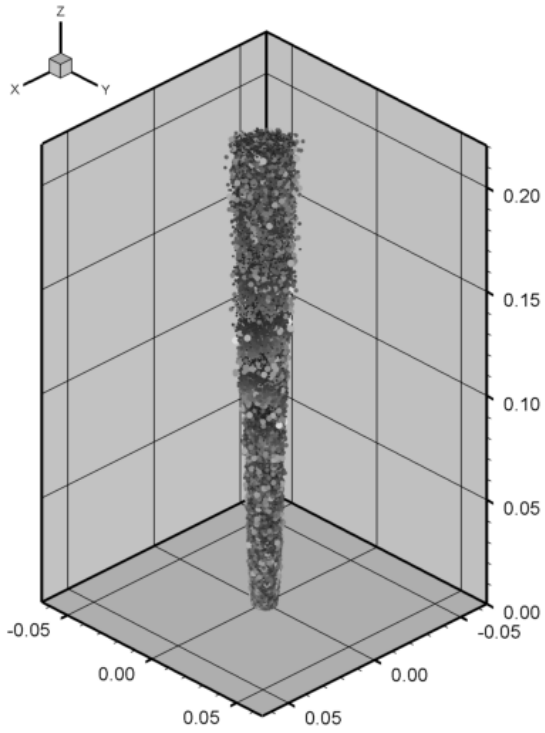

Figure 4: Visualisation of the instantaneous droplets distribution - colors of the markers and their sizes are related to the droplet diameters, $U_p = 0.05U_1,\ \alpha_p = 60^o$. Results obtained for **non-excited** jet.

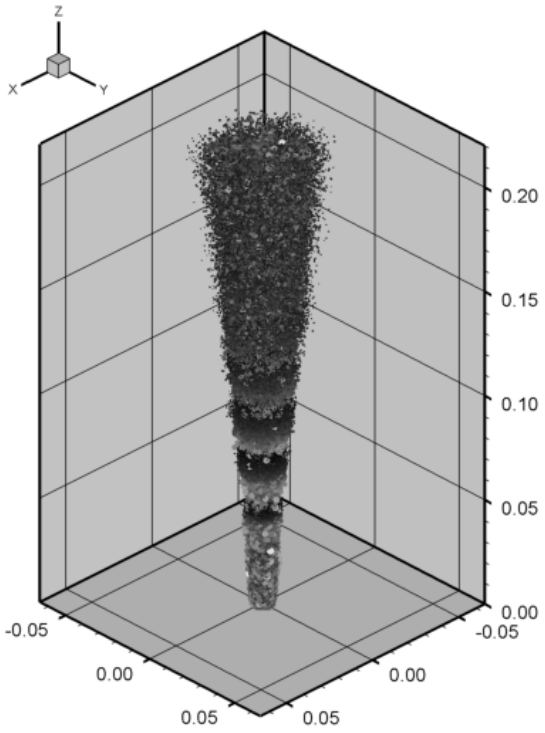

Figure 5: Visualisation of the instantaneous droplets distribution - colors of the markers and their sizes are related to the droplet diameters, $U_p = 0.05U_1,\ \alpha_p = 60^o$. Results obtained for **excited bifurcating** jet.

seen - this results were obtained for pure jet. The comparison of the obtained velocity profiles with experimental data (Lee and Reynolds, 1985) is shown in Fig. 3, where the results are presented normalized by the inlet jet velocity and the jet nozzle diameter. As one may observe agreement with experiment is very good confirming correctness of the LES simulation of the flowfield.

Due to limited size of the paper analysis of the results obtained for cases including droplets concentrates mainly on the influence of the excited jet on the droplets velocity and spreading rate of the injected spray. However, it is necessary to point out that the influence of the droplets on the flowfield by induced drag force (see Eq.(2)) is relatively small and it does not destroy the bifurcation phenomena. Figures 4 and 5 show instantaneous droplets distribution for the case with the inlet droplets velocity equal to 5% of the jet velocity and angle of injection equal to 60^o. In the cases where the inlet droplets velocity is small the angle of injetcion does not play a crucial role on the droplets distribution as they are mainly tracked by the gas phase flowfield. In the cases when the droplets velocity at the inlet is high then the inertia of the droplets is also high and in this situations the influence of the gas phase on the droplets distribution is relatively small. In Fig. 4 and 5 one may see that for the non-excited jet the spreading rate of the spray is relatively small and in fact it is smaller than spreading rate of the jet flow. In case of the excited jet presented in Fig. 5 one may observe that starting from approximately 2.5 jet diameters from the inlet the droplets distribution is affected by the excitation. When the inlet droplets velocity in the region close to the nozzle is small then the droplets accelerate tracked by the jet and their position is affected by the vortex rings resulting due to excitation. This phenomenon is well seen in Fig. 6 and 7 showing contours of the droplets diameter in the so-called bisecting and bifurcating planes. The bifurcating plane is the cross-section plane in the direction of the helical forcing while the bisecting plane is perpendicular to the bifurcating plane. In Fig. 6, presenting solution in bisecting plane, one may observe that the distribution of droplets is 'symmetric' with respect to the jet axis. In bifurcating plane (Fig. 7) we may see the effect of helical forcing which causes that the droplets distribution follows the alternate paring of the jet vortex rings which in this case are amplified by the excitation.

In the region close to the inlet the increase of the droplets inertia is caused mainly by the axial velocity of the gas phase which is the main source of the droplets movement. Therefore, further downstream the increased inertia of the accelerating droplets causes that the droplets are less affected by the gas phase and we can observe that the liquid phase leaves the main streams of the gas phase approximately $5-6$ jet diameters from the inlet. The helical disturbances caused by excitation grow starting from the inlet and in the region $5-6$ jet diameters downstream they are already strong enough to separate the gas phase into two bifurcating branches. However, these disturbances are not able to divide the liquid phase and as a result we observe three streams: two branches of the bifurcating gas phase and the liquid phase in the middle.

Figures 8 and 9 show the profiles of the mean axial and radial velocity of the droplets in bifurcating plane at 9 jet diameters from the inlet plane for the computations performed with and without excitation. These results concern the solutions presented in Fig. 4 and Fig. 5, i.e. the parameters of injection are $U_p = 0.05U_1,\ \alpha_p = 60^o$. The excitation of the jet causes that profile of the droplets axial velocity is wider

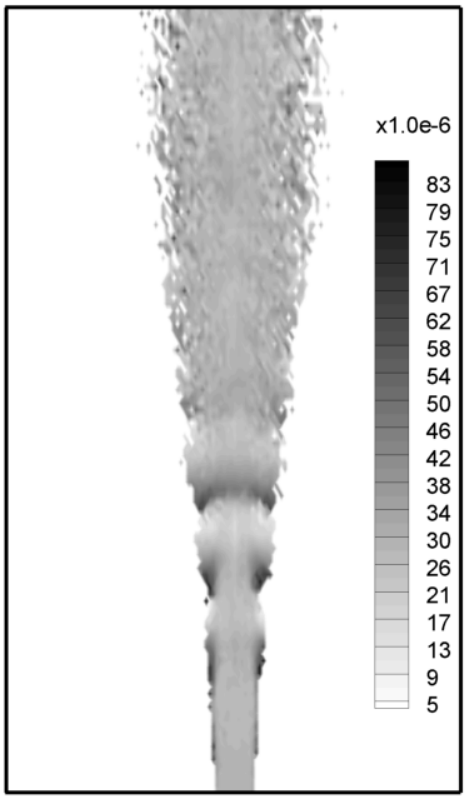

Figure 6: Contours of the droplets diameters in bisecting plane, $U_p = 0.05U_1$, $\alpha_p = 60^o$. Results obtained for **excited bifurcating** jet.

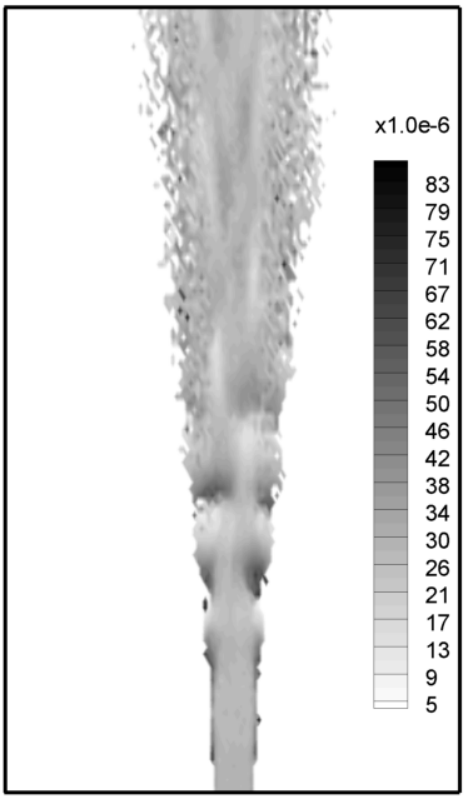

Figure 7: Contours of the droplets diameters in bifurcating plane, $U_p = 0.05U_1$, $\alpha_p = 60^o$. Results obtained for **excited bifurcating** jet.

comparing to non-excited case but the levels of the maximum velocity are more or less the same in both cases. Considerable differences occurs in the case of the radial velocity where for the excited jet the maximum values of droplets velocity are approximately three times higher comparing to the non-excited case. This causes that the spreading rate of the spray is higher when the jet is excited. The profiles of the mean droplets diameters, presented in Fig. 10, show qualitative differences between analyzed cases. For computations without excitation the large droplets occur in external layer of the spray while in the case with excitations the distribution of the droplets diameters is almost uniform, however in this case we can find three maxima: one in the center of the spray and two in the external layer. This phenomenon is probably caused by helical disturbances which try to move large droplets existing in the external layer (see Fig. 6 and 7) toward the jet axis. The results obtained for the case with the inlet spray velocity equal to 10% of the jet velocity are qualitatively very similar to those presented for $U_p = 0.05U_1$, for both angles of injection. Considerably different are the results obtained for $U_p = U_1$, in this case the effect of excitation is almost not seen and this is caused by large inertia of the droplets at the inlet to the computational domain.

CONCLUSIONS

The results obtained show that application of the low energetic small amplitude excitation of the gas phase results in bifurcating jet. In such conditions the downstream characteristic of the droplets properties (velocity, diameters distribution) injected in the center of the jet nozzle are considerably different comparing to the non-excited cases. The spreading rate of the spray is higher that means that at relatively small cost one may effectively influence the mixing properties. This effect was observed when the velocity of the injected droplets was small. Computations of the evaporating spray in non-isothermal conditions are planned for future studies where we expect to observe better evaporation rate resulting from improved mixing of the liquid and gas phase.

The support for the research was provided within statutory funds BS-1-103-301/2004/P. The authors are grateful to the TASK and Cyfronet Computing Centers (Poland) for ∗ *access to the computing resources.*

REFERENCES

Canuto C., Hussaini M.Y., Quarteroni A. and Zang T.A. (1988), *Spectral methods in fluid dynamics*, Springer-Verlag.

Crow S.C. and Champagne F.H. (1971), 'Orderly structure in jet turbulence', *Journal of Fluid Mechanics* **48**, 547–691.

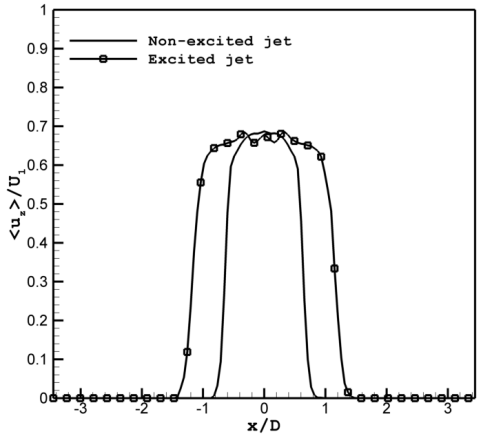

Figure 8: Profiles of the mean axial droplets velocity in bifurcating plane at 9 jet diameters from the inlet, $U_p = 0.05U_1,\ \alpha_p = 60^o$.

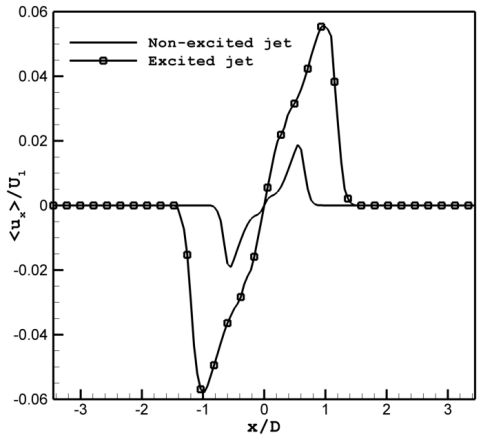

Figure 9: Profiles of the mean radial droplets velocity in bifurcating plane at 9 jet diameters from the inlet, $U_p = 0.05U_1,\ \alpha_p = 60^o$.

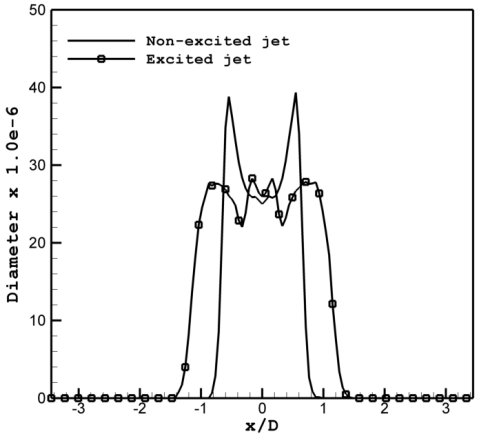

Figure 10: Profiles of the mean droplets diameters in bifurcating plane at 9 jet diameters from the inlet, $U_p = 0.05U_1,\ \alpha_p = 60^o$.

da Silva C.B. and Metais O. (2002), 'Vortex control of bifurcating jets: A numerical study', *Physics of Fluids* **14**(11), 3798–3819.

Ducros F., Comte P. and Lesieur M. (1996), 'Large-eddy simulation of transition to turbulence in a boundary layer developing spatially over a flat plate', *Journal of Fluid Mechanics* **326**, 1–36.

Fletcher C.A.J. (1991), *Computational Techniques for Fluid Dynamics*, Springer-Verlag.

Jones W.P. and Sheen D.-H. (1999), 'A probability density function method for modelling liquid fuel sprays', *Flow, Turbulence and Combustion* **63**, 379–394.

Lee M. and Reynolds W.C. (1985), Bifurcating and blooming jets, Technical Report TF-22, Stanford University.

Lefebvre A.H. (1989), *Atomization and sprays*, Hemisphere Publishing Corporation.

Lele S.K (1992), 'Compact finite difference with spectral-like resolution', *Journal of Computational Physics* **103**, 16–42.

Metais O., Lesieur M. and Comte P. (1999), *Transition, turbulence and combustion modelling*, KLUWER Academic Publisher, chapter Large-eddy simulations of incompressible and compressible turbulence.

Parekh D., Leonard A. and Reynolds W.C. (1988), Bifurcating jets at high Reynolds number, Technical Report TF-35, Stanford University.

Reynolds W.C., Parekh D.E., Juvet P.J.D. and Lee M.J.D. (2003), 'Bifurcating and blooming jets', *Annual Review of Fluid Mechanics* **35**, 295–315.

Sagaut P. (2001), *Large eddy simulation for incompressible flows*, Springer.

Tyliszczak A. and Boguslawski A. (2006), LES of the jet in low Mach variable density conditions, *in* 'Direct and Large Eddy Simulations VI', ed. Geurts B.J. Metais O. Lamballais E., Friedrich R., ERCOFTAC, Springer, pp. 575–582.

Tyliszczak A. and Boguslawski A. (2007), *LES of variable density bifurcating jets*, Lecture Notes in Computational Science and Engineering - Complex Effects in Large Eddy Simulations, Springer, pp. 273–288.

Williamson J. H. (1980), 'Low-Storage Runge-Kutta Schemes', *Journal of Computational Physics* **35**, 48–56.